European Journal of Technique

journal homepage: https://dergipark.org.tr/en/pub/ejt

Vol.15, No.2, 2025

Research Article

Design of a PV-Powered Wireless EV Charger Employing PDM-Controlled MPPT

Cem KUTLU[1*], **Harun OZBAY**[2]

[1*]Bandırma Onyedi Eylül Üniversitesi, Mühendislik ve Doğa Bilimleri Fakültesi, Bandırma/Balıkesir, Türkiye (e-mail: cem.kutlu@ogr.bandirma.edu.tr)
[2] Bandırma Onyedi Eylül Üniversitesi, Mühendislik ve Doğa Bilimleri Fakültesi, Bandırma/Balıkesir, Türkiye (e-mail: hozbay@bandirma.edu.tr)

ARTICLE INFO

Received: Oct., 16. 2025
Revised: Nov., 28. 2025
Accepted: Dec, 03. 2025

Keywords:
Resonant Converters
Electric Vehicles
Soft Switching
MPPT
PV Systems

Corresponding author: *Cem Kutlu*

ISSN: | e-ISSN:

DOI: https://doi.org/10.36222/ejt.1804687

ABSTRACT

This paper proposes the design and co-simulation of a Solar-Powered Wireless Electric Vehicle (EV) Charger employing a Pulse Density Modulation (PDM) controlled Maximum Power Point Tracking (MPPT) algorithm for enhanced efficiency and precise power flow management. The system is engineered to efficiently harvest energy from a high-power Photovoltaic (PV) array and transfer it wirelessly to an EV battery. The entire power stage, which includes the PV array, Series Resonant Inverter, Wireless Power Transfer (WPT) coils, rectifier, and battery load, is modeled in PSIM. Conversely, the Perturb and Observe (P&O) MPPT algorithm and the generation of the control signals via a 16-level Irregular PDM technique are implemented in MATLAB/Simulink using a co-simulation methodology. The system was tested under varying solar irradiance levels. Results confirm the PV array's maximum power was successfully tracked, while the 16-level Irregular PDM control method ensured precise power flow regulation. Crucially, the PDM strategy facilitated reliable Zero Voltage Switching (ZVS**)** operation, which is key to guaranteeing the high overall efficiency of the wireless charging process.

1. INTRODUCTION

With the gradual increase in the world's population, the necessity for energy is rising, mainly due to industrialization, advanced technology and manufacturing. Fossil fuels, which have a crucial role in satisfying the world's energy demand, cannot continue to fulfil the requirements for extended periods with their actual reserves. Over and above, power stations that use fossil fuels for the generation of electrical energy have a very negative effect on our planet [1], [2], [3]. The finite nature and environmental impact of fossil fuels has been the driving force behind research into renewable energy sources, particularly solar power in recent years.

In addition to solar energy, electric vehicles (EVs) are also perceived as a viable solution to lower carbon emissions. Recent developments in battery and power electronics technology have led to substantial growth in the market for electric cars. The number of EVs on the roads is steadily increasing consequently [4]. When it comes to capturing energy from renewable sources and transforming it for the end user, power electronic converters play a vital role. Furthermore, power electronic converters contribute significantly to the efficiency of EVs. Advanced power electronic converters are needed to meet their diverse power conversion and control requirements [5]

The integration of PV technologies into EV charging systems present a high potential owing to the latest strides. Notwithstanding the dominance of plug-in chargers, charging of EVs with WPT is emerging an attractive choice instead of conductive charging due to its sturdy nature and secure charging experience [6].

The inductively coupled WPT system operates based on the same fundamental mechanism as an ordinary transformer. However, it uses transmitting and receiving coils with low coupling, apart by an air gap [7]. This leads to a high leakage flux of noncoupled coils compared to conventional transformers, and the efficiency can be significantly reduced [8]. The coupling coefficient and load resistance in WPT systems are frequently uncertain and variable in numerous applications, affecting both output power and system efficiency significantly, particularly during dynamic applications. For instance, if the coupling coefficient decreases due to coil misalignment or if the actual load resistance no longer matches the optimum value, the efficiency can be significantly reduced [9]. Moreover, while power transmission is taking place wirelessly, a magnetic flux occurs in the coils, which results in the WPT system producing an electromagnetic force.

Hence, it is essential to minimize leakage flux due to its potential harmful effects on human health. In order to both restrict the magnetic leakage flux and increase the efficiency, it would be sensible to raise the magnetic coupling coefficient by means of a convenient coil design [7].

There is increasing research interest on integrating renewable energy in WPT systems, with a particular emphasis on utilizing solar energy for both static and dynamic charging of EVs [10]. A solar-powered WPT system using dual phase shift control is proposed in [11] to facilitate the integration of solar energy into the EV charging infrastructure. A prototype of 1kW has also been developed. In [12], a different solar power system with a three-phase wireless power transfer system for EV charging is examined and constructed. A power management algorithm was proposed in [13] that efficiently monitors the contribution of various energy sources to a vehicle's charging process. Designed in [14], the solar-powered e-bike charging station has wireless charging capabilities. The evaluation and analysis of PV powered dynamic wireless charging systems is detailed in [15]. A WPT system that transfers energy from a solar battery to the rover body has been proposed in [16]. Proper quantity of energy is provided by switching a step-down converter between MPPT and buck mode

Research on WPT has mainly focused on three aspects: coupling, compensation topologies, and control techniques. Nevertheless, the implementation of an appropriate control strategy in the WPT system remains critical to ensure optimal efficiency of the high frequency inverter. The accuracy and efficiency of WPT systems are highly dependent on the performance of converters and the control strategy [17].

An EV battery charger is developed in [18] using PSM for a full-bridge inverter in a WPT system. However, ZVS is not achieved, resulting in increased system loss. The PSM control method explained in [19], also does not provide ZVS while it alters the phase-shift angle to regulate the output. A comparative study of primary side FM control versus secondary side PWM control to achieve constant current and constant voltage charging is carried out using the 3kW WPT topology in [20].

Numerous control techniques have been examined for WPT systems to achieve high efficiency in the transfer of power to the recipient. Pulse width modulation (PWM), phase shift modulation (PSM) and pulse density modulation (PDM) are commonly discussed control methods in researches. [21].

PDM is typically favoured for high frequency inverter designs on account of its efficiency enhancement. However, it is important to acknowledge that PDM may produce oscillations in inverter output current or even result in system failures at poor quality factor or low-load cases [21]. In particular, its ability to provide soft switching conditions at various power levels means that it remains a viable choice for WPT systems. In addition, PDM is utmost effective in WPT systems with higher quality factors [22]

In PDM control, without changing the switching frequency and turn-on time, power control is achieved by deleting certain control pulses based on command sequences. As the quantity of deleted control pulses rises, the output power of the converter diminishes [23] The output power can be extensively controlled by changing the number and arrangement of transmission pulses applied to the power switches.

PDM-MPPT controlled WPT system powered by a PV module is proposed in [24] and the irregular 16 PDM technique implemented with the IC algorithm was used to track maximum power. WPT efficiency is stated to be %90 while MPPT efficiency is over %98. A novel harmonic-based Pulse Density Modulation technique is proposed in [25] to reduce HFI output current ripple in IPT systems, improving system efficiency at light loads. Enhanced and improved PDM strategies, as proposed in [26] and [21] respectively, were utilized in this study and compared to the traditional irregular PDM method in terms of efficiency and resonance current frequency components.

The achievements of this study can be listed as follows;

- A high-efficiency charging system for electric vehicles has been developed.
- High frequency WPT is used in the proposed system.
- The charging system is powered by PV panels with MPPT.
- High efficiency is attained through the utilization of a HFSRI.
- Power control of the resonant circuit is achieved by employing PDM technique.

The following sections of this study will provide information on the SRI, PDM control method, and the details of the designed system. Afterwards, the results of co-simulation of the power stage and control unit and the final evaluation will be presented.

2. RESONANT CONVERTER AND PDM CONTROL

2.1. Series Resonant Inverter (SRI)

A full-bridge series resonant inverter, one of the most preferred topologies in WPT systems, is shown in Figure 1(a). The circuit consists of a DC voltage source, 4 switches and a resonance tank.

The circuit features three distinctive modes of operation as illustrated in Figure 1(b), (c) and (d). The first mode provides a V_{DC} voltage at the output when switches S_1 and S_4 are in a conducting state. The second mode, when switches S_2 and S_3 are on, results in a $-V_{DC}$ voltage at the output. Finally, switches S_2 and S_4 are conducting, resulting in a zero output since there is no connection between the input and output in the third mode. In this mode, the current passes through diodes D_2 and D_4, which are connected to switches S_2 and S_4, completing the circuit [3].

The energy stored within the resonance elements is dissipated by the effective resistance, resulting in a damped oscillation current. The maintenance of this current form relies on selecting a sufficient quality factor. [27]

The circuit's basic equations, representing the resonant frequency and quality factor are provided in equation (1) and (2) respectively.

$$f_r = \frac{1}{2\pi\sqrt{L_r C_r}} \tag{1}$$

$$Q = \frac{1}{R}\sqrt{\frac{L_r}{C_r}} \tag{2}$$

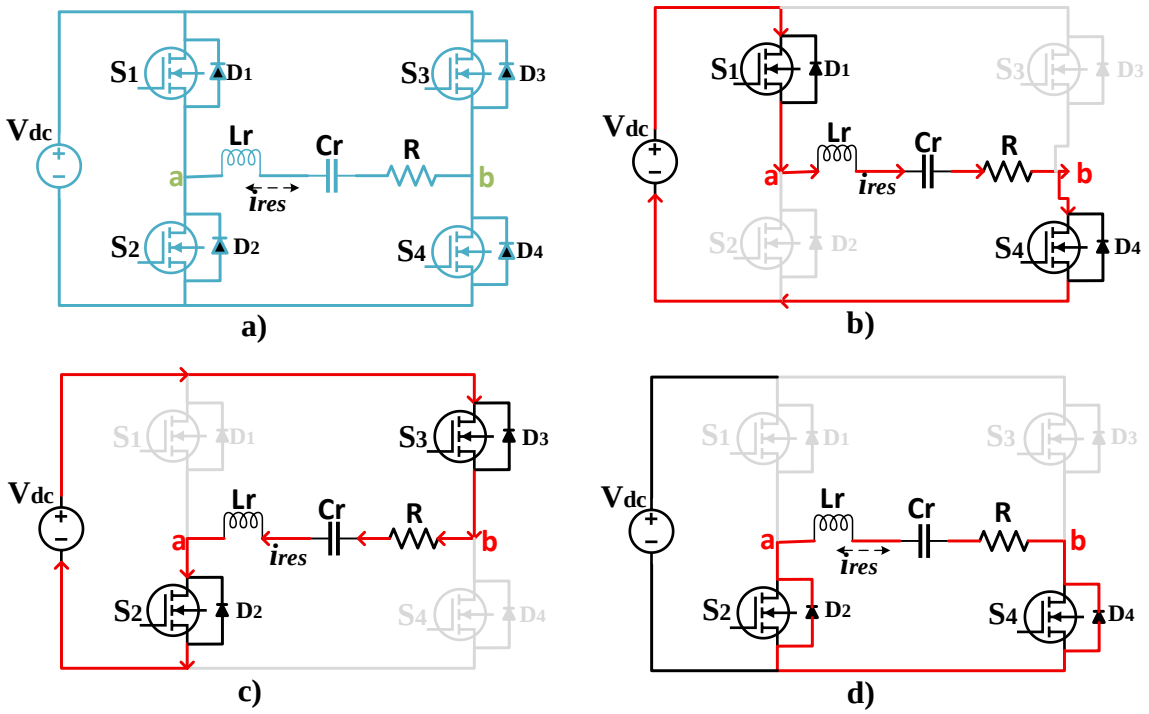

Figure 1. Full bridge SRI and switching modes a) equivalent circuit b) Mode I c) Mode II d) Mode III

In the case of Q > 1, the current oscillates in a sinusoidal form. The resonance current and average power are obtained using Equations (3) and (4). The resonant current is denoted by $i(t)$ while its envelope is represented by $i_E(t)$ [23]

$$i(t) = i_E(t)\, sin\, w_r t \tag{3}$$

$$P = \frac{1}{T}\int_0^T V_{ab}\, i(t)dt \tag{4}$$

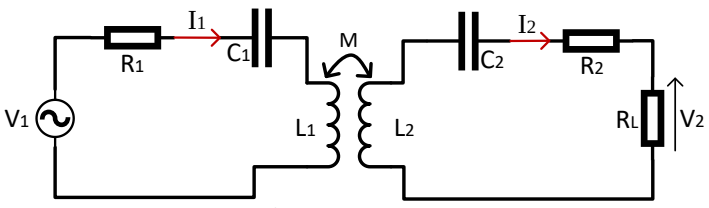

Figure 2. Equivalent model of the series-series compensated WPT system.

The charging system utilizes an SRI which is positioned on the ground side of the charger, to generate a high-frequency alternating voltage. This voltage is subsequently applied to the transmitter coil. The resultant square wave current generates a time-varying magnetic field. Through mutual coupling between the transmitter and receiver coils, this magnetic field successfully induces a voltage in the vehicle-side coil. The induced voltage is then rectified and delivered to power the load, which is the EV battery pack [28]

Figure 2 illustrates the equivalent circuit configuration for the WPT model. In this model, the parameters L, R, and C represent the inductance, resistance, and capacitance, respectively. The subscripts 1 and 2 are used to denote the parameters belonging to the primary (ground) and secondary (vehicle) sides, respectively. Based on this equivalent circuit model for the series-series (SS) topology, the system can be further defined as follows:

$$\begin{bmatrix} V_1 \\ 0 \end{bmatrix} = \begin{bmatrix} Z_1 & j\omega M \\ j\omega M & Z_2 \end{bmatrix} \begin{bmatrix} I_1 \\ I_2 \end{bmatrix} \tag{5}$$

$$Z_1 = R_1 + j\omega L_1 + \frac{1}{j\omega C_1} \tag{6}$$

$$Z_2 = R_2 + R_L + j\omega L_2 + \frac{1}{j\omega C_2} \tag{7}$$

Hence, it can be inferred that the transmitter and receiver currents in the equivalent circuit are represented by equations (8) and (9).

$$I_1 = \frac{V_1 \cdot Z_2}{(\omega M)^2 + Z_1 \cdot Z_2} \tag{8}$$

$$I_2 = \frac{j\omega M V_2}{(\omega M)^2 + Z_1 \cdot Z_2} \tag{9}$$

The reflected impedanc Z_r and the corresponding input impedance observed from the transmitter side are defined in equations (10) and (11).

$$Z_r = \frac{-j\omega M I_2}{I_1} = \frac{\omega^2 M^2}{Z_2} \tag{10}$$

$$Z_{in} = Z_1 + \frac{\omega^2 M^2}{Z_2} \tag{11}$$

At the resonant frequency, I_1 and power transfer efficiency η can be expressed by equation (12) and (13) respectively.

$$I_1 = \frac{V_1(R_2 + R_L)}{(\omega M)^2 + R_1(R_2 + R_L)} \quad (12)$$

$$\eta = \frac{P_{out}}{P_{in}} = \frac{R_L\,(\omega M)^2}{(R_2 + R_L)\,(R_1\,(R_L + R_2) + (\omega M)^2)} \quad (13)$$

2.2. Pulse Density Modulation (PDM)

The traditional irregular PDM technique regulates the magnitude of the output power by adapting the on/off ratio of the control pulses within a defined period, effectively modifying the time of energy transfer to the load. A PDM period T_{Pdm} is composed of N resonant periods, where each resonant period is defined as T

Within a PDM cycle, the inverter circuit actively delivers energy to the load during the T_{on} interval. Subsequently, during the T_{off} interval, the inverter ceases operation, and the load energy dissipates through free oscillation. The Pulse Density (PD), which is the key control parameter can be expressed as T_{on}/T_{PDM}. By controlling the Pulse Density PD, the output power can be precisely regulated. [29]

PDM control methods are fundamentally categorized into two groups based on the pattern length of the control pulses within a period: regular and irregular. While the regular PDM method distributes control pulses in a simple, consistent sequence, the irregular PDM technique distributes control pulses in a non-uniform sequence. This irregular distribution maintains a more even flow of current throughout the period, preventing the current from dropping to zero before the arrival of the next pulse. [30]

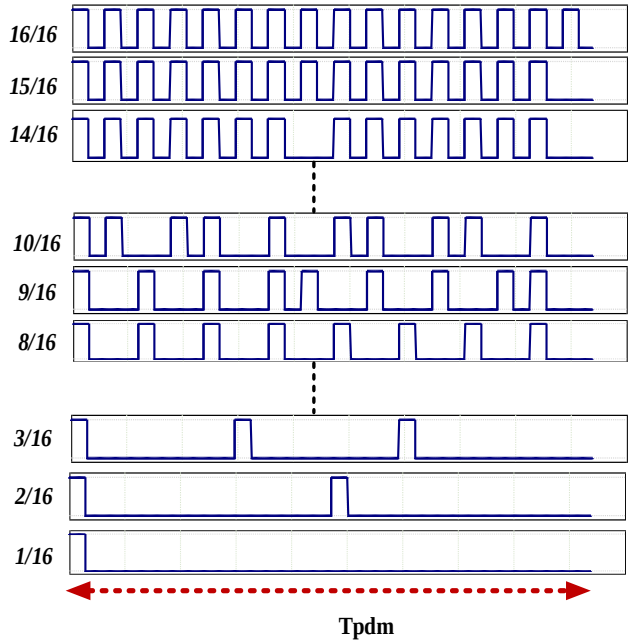

Figure 3. Swtching patterns of irregular PDM for N=16

This particular characteristic of irregular PDM offers significant benefits:

- It avoids high peak currents and voltage stresses on the components, allowing for the use of lower-rated elements, which consequently reduces the overall system cost [30].
- It significantly reduces the amplitude of low-frequency harmonics in the system [30] [31].

Due to these superior advantages in reducing stress and mitigating harmonics, the irregular PDM technique was selected for this study. The $N = 16$ irregular PDM switching patterns utilized are specifically illustrated in Figure 3.

The sequence of rows illustrates 16 resonant cycles that have been configured to regulate the inverter switches. When the maximum PDM length N, is set to 16, the pulse density, denoted by PD, fluctuates within the range of 1/16 to 16/16. In the case of 1/16, the lowest power is achieved; conversely, the maximum power is provided in 16/16 [32]

3. DESCRIPTION AND MODELLING OF PROPOSED SYSTEM

The comprehensive system design is visually depicted in Figure 4. To effectively manage the high-frequency power control dictated by the PDM technique across various power levels, a co-simulation approach was employed. This methodology allows the system to leverage the respective strengths of two distinct simulation tools: The physical power electronics components—including the inverter and WPT system—were accurately modeled and analyzed in the PSIM software environment.

TABLE I
SPECIFICATIONS OF THE PV PANEL.

Parameter	Symbol	Value
Maximum Power	P_{max}	$550W$
Voltage at maximum power	V_{mpp}	$32.57V$
Current at maximum power	I_{mpp}	$16.90A$
Open circuit voltage	V_{oc}	$41.075V$
Short circuit current	I_{sc}	$18.49A$

Conversely, the complex control algorithms—specifically the Perturb & Observe (P&O) MPPT and the PDM signal generation logic—were implemented using the powerful computational capabilities of MATLAB/Simulink. This rigorous co-simulation provides a highly realistic platform for verifying the interaction between the high-speed power conversion stage and the dynamic control loop, which is crucial for systems utilizing advanced switching techniques like PDM.

The power circuit is fundamentally composed of a PV module—which includes fourteen series-connected panels—a full-bridge series resonant inverter, a resonant tank incorporating the transmitter coil, the receiver coil (on the EV side), a full-wave rectifier, a filter, and the final load (EV battery). The PV array utilizes the TT550-108PM12 panel model with a 108-cell monocrystalline structure, the technical specifications of which are provided in Table 1. With each panel rated for a maximum output of $550W$, the series connection results in a total maximum PV array power of $7.7kW$. The circuit parameters of the designed system are given in Table 2.

Recognizing that the power output of PV panels inherently fluctuates due to environmental factors, a precise Maximum Power Point Tracking (MPPT) algorithm is imperative to maximize operational efficiency

The system was tested under three distinct irradiance levels to achieve varying power outputs, while the cell temperature was held constant at 25℃.

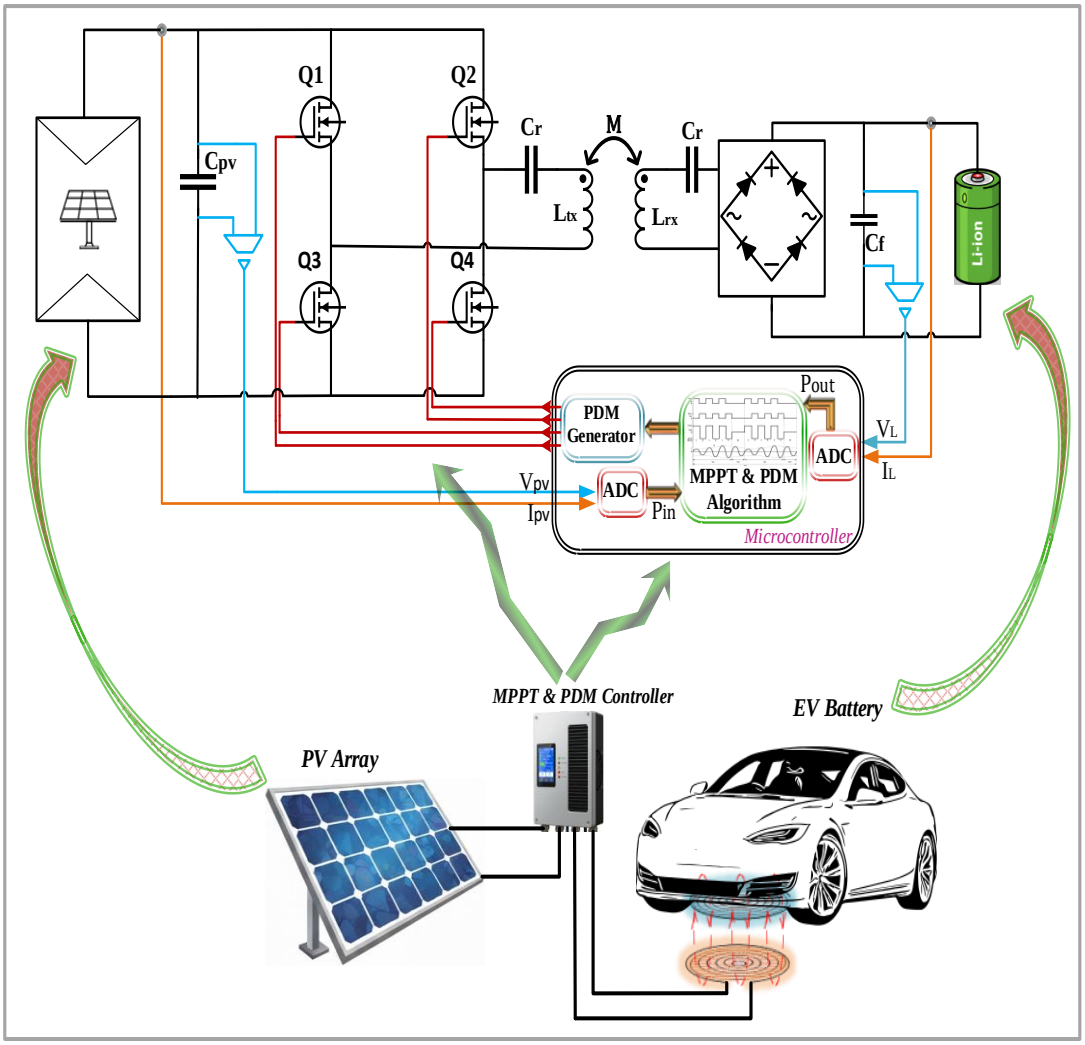

Figure 4. Design of solar powered wireless EV charging system.

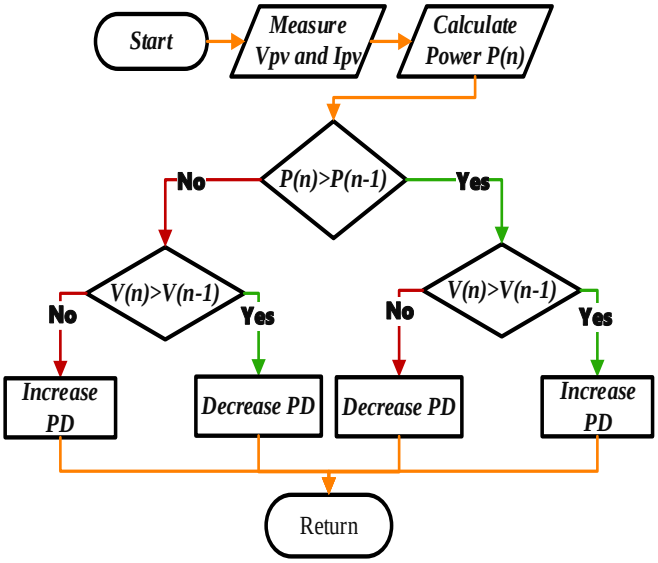

Figure 5. Flowchart of the MPPT algorithm

To achieve robust MPPT, the widely used P&O algorithm, enhanced with PI control, was implemented. The P&O algorithm is highly preferred due to its simplicity and proven efficiency, capable of consistently locating the Maximum Power Point (MPP) regardless of external factors [31]. The operational steps of the algorithm are detailed in the flowchart presented in Figure 5, and its integration with the PI control is illustrated in the block diagram in Fiure 6. The P&O method works by calculating the current power from the measured PV voltage and current, then comparing this value to the previous power. An increase in power triggers an incremental perturbation (ΔV) in the reference voltage (Vref). Conversely, a decrease in power reverses the perturbation, driving the system towards the MPP and sustaining continuous tracking oscillation around that optimal point [32]

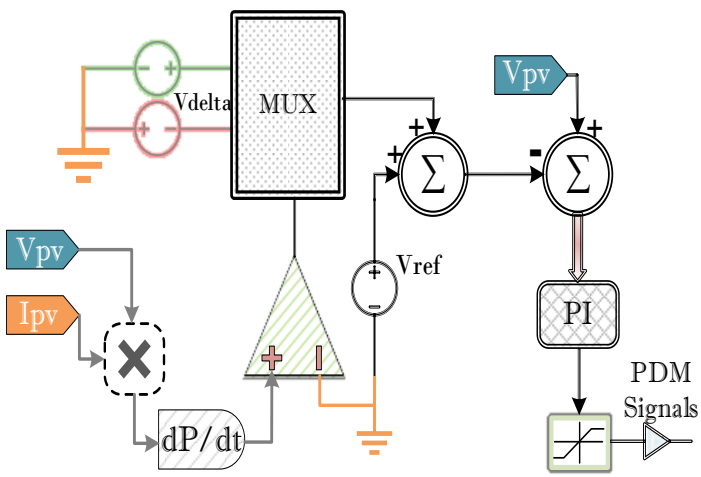

Figure 6. Block diagram of the PI controlled P&O MPPT algorithm

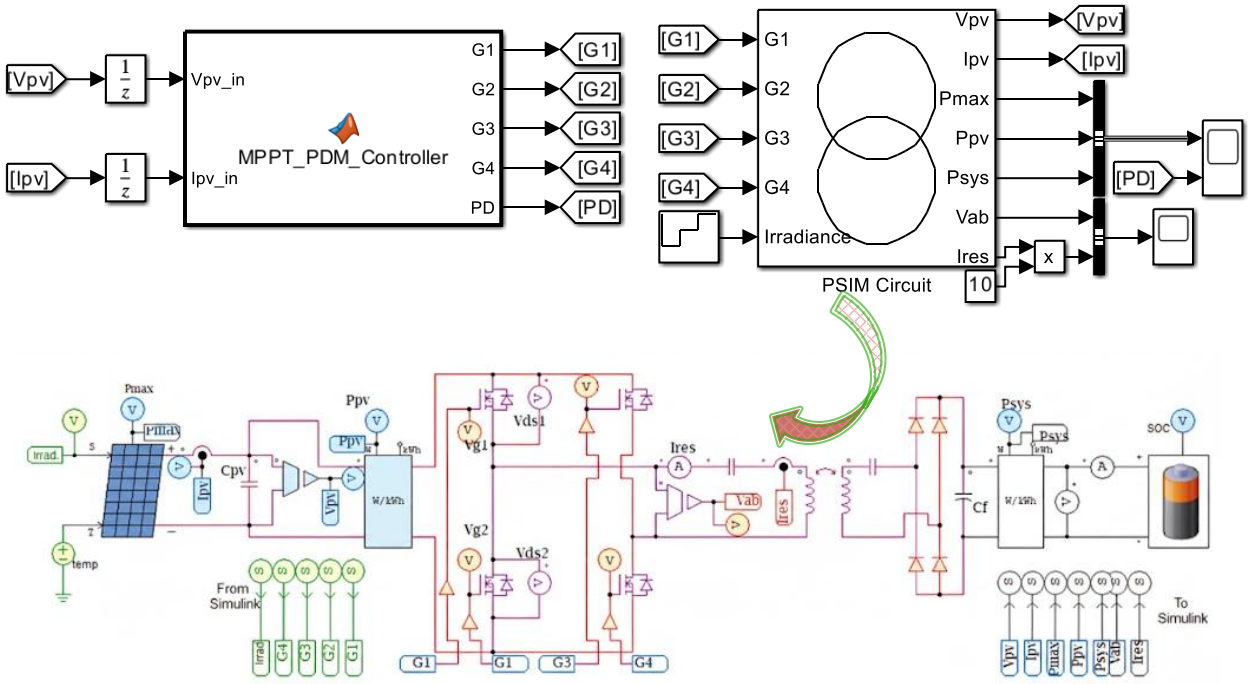

Figure 7. Co-simulation design of Simulink&PSIM for the proposed system

4. SIMULATION RESULTS

The comprehensive design of the proposed system was executed using a co-simulation approach, with the full architecture depicted in Figure 7. The control logic, which encompasses the MPPT algorithm and PDM signal generation, was developed in MATLAB/Simulink. Conversely, the physical power electronics stage—modeled in the PSIM software environment—includes the PV module, input filter, resonant inverter, the magnetically coupled coil pair (WPT), full-wave rectifier, and the EV battery load. Crucially, to ensure high fidelity between the simulation outcomes and potential real-world performance, all integrated components were meticulously modeled using specifications derived from their datasheets, rather than assuming any ideal characteristics.

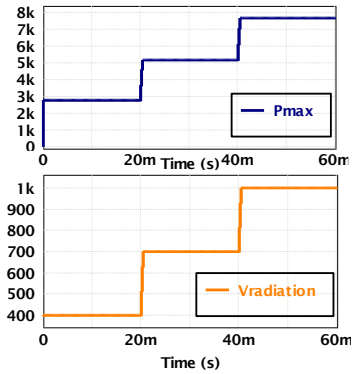

Figure 8. Maximum power of PV Array due to irradiance levels

The simulation was conducted over a 60 ms period, during which the Photovoltaic (PV) module was subjected to step changes in irradiance. Specifically, irradiance values of $400W/m^2$, $700W/m^2$, and $1000W/m^2$ were applied sequentially at 20 ms intervals. Correspondingly, the PV system generated maximum power levels of approximately $2.8kW$, $5.2kW$, and $7.7kW$ during these respective time frames as shown in Figure 8.

The P&O MPPT algorithm, implemented using a MATLAB function block, was designed to efficiently track and maintain maximum power transfer from the PV system. This transfer is achieved by applying soft switching at the inverter's resonance frequency of $85kHz$.

The control relies on a 16-level ($N = 16$) PDM scheme. Based on the instantaneous power value received from the PV system, the control algorithm automatically determines the required Pulse Density (PD) and generates the corresponding PDM signals to drive the resonant inverter switches. Maximizing the overall system efficiency is critically dependent on the algorithm's success in determining the suitable PD for each power level instantaneously.

The selection of the PDM length, N=16, represents a strategic trade-off between output power resolution and the dynamic response of the control loop. While a larger frame length (N) offers finer granularity in power modulation—essential for minimizing steady-state error during Maximum Power Point Tracking (MPPT)—it inevitably introduces lower-frequency sub-harmonics and can delay the system's transient response. Conversely, a smaller N yields faster response times but results in coarser power regulation steps, which may lead to significant oscillations around the MPP. Consequently, N=16 was chosen to provide adequate control precision (offering power increments of approximately 6.25%) while ensuring system stability and rapid convergence under varying irradiance conditions

For clarity in presenting the results, the following variables are illustrated in the figures pertaining to the designed system: Pmax is defined as the maximum theoretical power that the PV module can produce, Ppv represents the actual power obtained from the PV array via the MPPT algorithm, Psys denotes the final output power transferred to the load.

As demonstrated in Figure 9, the simulation outcomes from the PI-controlled P&O MPPT algorithm clearly validate the algorithm's effectiveness. The graphs illustrate the consistent maintenance of maximum power transfer despite the rapid variation in solar irradiance, confirming the robust performance of the proposed control architecture.

TABLE II
CIRCUIT PARAMETERS OF THE DESIGNED SYSTEM

Circuit Paramters	Value
$Lr_{1,2}$	116.8µH
M	35µH
$Cr_{1,2}$	30nF
f_r	85kHz
(coupling coef.) k	0.3
(PI) K_p	120
(PI) K_i	20

TABLE III
SIMULATION RESULTS FOR MPPT AND SYSTEM EFFICIENCIES

Irradiance	Pmax	Ppv	Psys	η_{MPPT} (Ppv/Pmax)	η_{SYS} (Psys/Ppv)
$400W/m^2$	$2.81kW$	$2.78kW$	$2.74kW$	%98,93	%98,56
$700W/m^2$	$5.22kW$	$5.20kW$	$5.15kW$	%99,61	%99,03
$1000W/m^2$	$7.70kW$	$7.61kW$	$7.54kW$	%98,83	%99,08

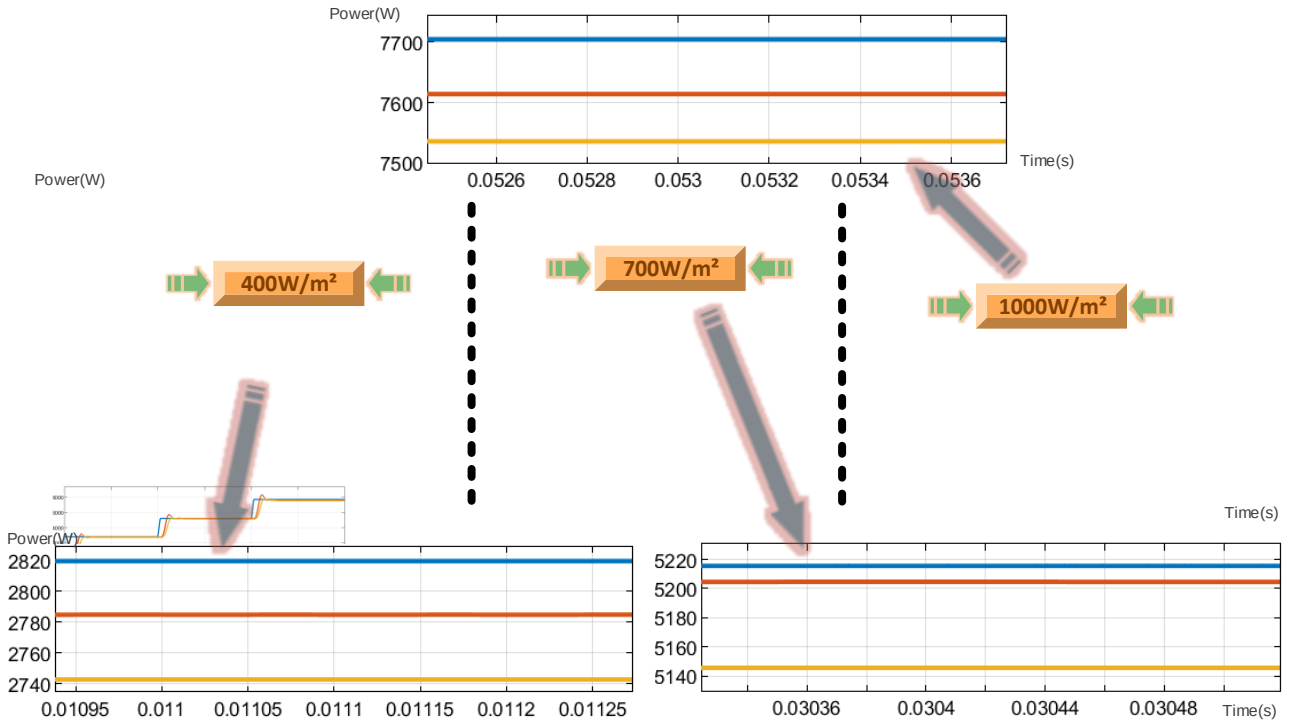

Figure 9. Maximum and achieved power of PV Array, and the power transmitted in the system.

Figure 10 provides a comprehensive illustration of the inverter output voltage (V_{ab}) and the resonance current (I_{res}). As is evident from the detailed view of the voltage and current signals across all tested irradiation levels, the system successfully operates under ZVS conditions. This confirmation is crucial as it demonstrates that the Irregular PDM strategy effectively maintains the inverter at full resonance, thereby minimizing switching losses and ensuring high efficiency. The resultant performance metrics, including both the MPPT efficiency and the overall system efficiency, are summarized in Table 3.

5. CONCLUSION

The co-simulation methodology, leveraging the strengths of PSIM for power electronics and MATLAB/Simulink for control logic, proved to be an effective tool for the comprehensive design and testing of the integrated system. The results confirm that the MPPT algorithm consistently achieved exceptional performance in tracking the maximum power from the PV array. Under all tested irradiance conditions ($400W/m^2$, $700W/m^2$ and $1000W/m^2$), the algorithm maintained approximately an average MPPT efficiency of 99%. Furthermore, the implementation of the 16-level Irregular PDM technique for the Series Resonant Inverter provided precise power flow control while maintaining Zero Voltage Switching (ZVS) conditions, which is essential for minimizing switching losses. This successful integration resulted in a high power transfer efficiency for the WPT stage, reaching 98.56% at the lowest power level ($2.8kW$) and consistently reaching 99% at high power levels ($5.2kW$ and $7.7kW$). This validates the efficacy of PDM in achieving both precise power control and high-efficiency power delivery in solar-powered wireless charging applications. The system is designed and simulated at a power level of 7.7 kW, complying with the SAE J1772 Level 2 charging standard, demonstrating its suitability for real-world high-power EV charging applications.

Future work will involve optimizing the PDM resolution for further harmonic reduction and implementing a hardware prototype to validate these promising simulation results.

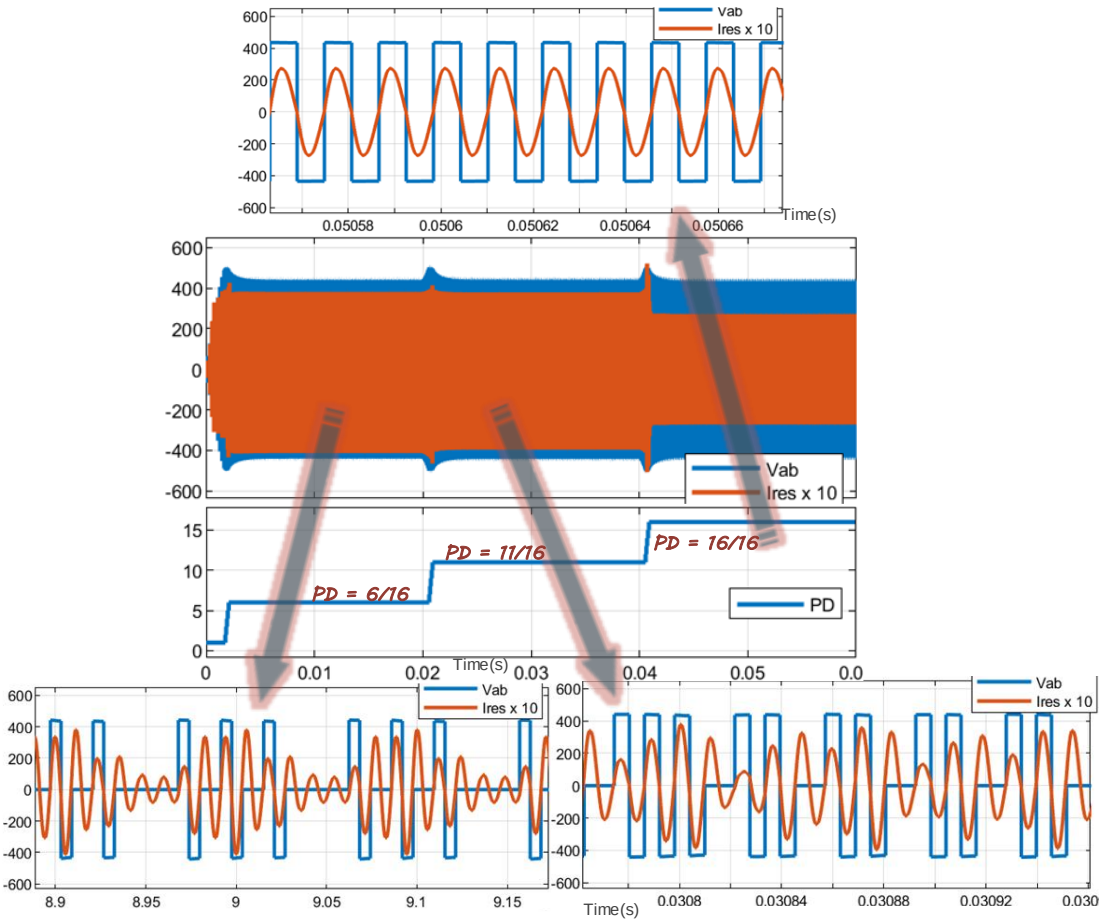

Figure 10. SRI output voltage-resonant current waveforms and PD selection of control algorithm for varying irradiance levels

REFERENCES

[1] V. Yenil and S. Cetin, "An Improved Pulse Density Modulation Control for Secondary Side Controlled Wireless Power Transfer System Using LCC-S Compensation," *IEEE Transactions on Industrial Electronics*, vol. 69, no. 12, pp. 12762–12772, 2022, doi: 10.1109/TIE.2021.3134059.

[2] G. Bal, S. Oncu, N. Ozturk, and K. Unal, "An Application of PDM Technique for MPPT in Solar Powered Wireless Power Transfer Systems," *10th IEEE International Conference on Renewable Energy Research and Applications, ICRERA 2021*, pp. 305–309, 2021, doi: 10.1109/ICRERA52334.2021.9598582.

[3] H. Özbay, "PDM-MPPT based solar powered induction heating system," *Engineering Science and Technology, an International Journal*, vol. 23, no. 6, pp. 1397–1414, 2020, doi: 10.1016/j.jestch.2020.06.005.

[4] Y. Yang, M. El Baghdadi, Y. Lan, Y. Benomar, J. Van Mierlo, and O. Hegazy, "Design methodology, modeling, and comparative study of wireless power transfer systems for electric vehicles," *Energies (Basel)*, vol. 11, no. 7, 2018, doi: 10.3390/en11071716.

[5] K. Kamalapathi, P. Srinivasa Rao Nayak, and V. K. Tyagi, "Design and implementation of dual-source (WPT + PV) charger for EV battery charging," *International Transactions on Electrical Energy Systems*, vol. 31, no. 11, pp. 1–29, 2021, doi: 10.1002/2050-7038.13084.

[6] W. Zhang *et al.*, "A Numerical Method to Reduce the Stray Magnetic Field Around the Asymmetrical Wireless Power Transfer Coils for Electric Vehicle Charging," *Journal of Electrical Engineering and Technology*, vol. 17, no. 3, pp. 1859–1871, 2022, doi: 10.1007/s42835-021-00948-6.

[7] A. Sagar *et al.*, "A Comprehensive Review of the Recent Development of Wireless Power Transfer Technologies for Electric Vehicle Charging Systems," *IEEE Access*, vol. 11, no. July, pp. 83703–83751, 2023, doi: 10.1109/ACCESS.2023.3300475.

[8] H. T. Nguyen *et al.*, "Review Map of Comparative Designs for Wireless High-Power Transfer Systems in EV Applications: Maximum Efficiency, ZPA, and CC/CV Modes at Fixed Resonance Frequency Independent from Coupling Coefficient," *IEEE Trans Power Electron*, vol. 37, no. 4, pp. 4857–4876, 2022, doi: 10.1109/TPEL.2021.3124293.

[9] J. Cai, X. Wu, P. Sun, J. Sun, and Q. Xiong, "Optimization Design of Zero-Voltage-Switching Control in S-LCC Inductive Power Transfer System Under Dynamic Coupling Coefficient," *Journal of Electrical Engineering and Technology*, vol. 16, no. 6, pp. 2937–2948, 2021, doi: 10.1007/s42835-021-00828-z.

[10] P. K. Joseph and D. Elangovan, "A review on renewable energy powered wireless power transmission techniques for light electric vehicle charging applications," *J Energy Storage*, vol. 16, pp. 145–155, 2018, doi: 10.1016/j.est.2017.12.019.

[11] Y. R. Kumar, D. Nayak, M. Kumar, and S. Pramanick, "A Solar Powered Wireless Power Transfer for Electric Vehicle Charging," *2022 IEEE Vehicle Power and Propulsion Conference, VPPC 2022 - Proceedings*, pp. 1–6, 2022, doi: 10.1109/VPPC55846.2022.10003449.

[12] R. Wiencek and S. Ghosh, "Comparative Analysis of Three-Phase Configurations for Efficient Wireless Electric Vehicle Charging," *Proceedings - 2023 IEEE 5th Global Power, Energy and Communication Conference, GPECOM 2023*, pp. 276–281, 2023, doi: 10.1109/GPECOM58364.2023.10175676.

[13] N. Mohamed, F. Aymen, Z. M. Ali, A. F. Zobaa, and S. H. E. Abdel Aleem, "Efficient power management strategy of electric vehicles based hybrid renewable energy," *Sustainability (Switzerland)*, vol. 13, no. 13, 2021, doi: 10.3390/su13137351.

[14] G. R. C. Mouli, P. Van Duijsen, F. Grazian, A. Jamodkar, P. Bauer, and O. Isabella, "Sustainable e-bike charging station that enables ac, dc andwireless charging from solar energy," *Energies (Basel)*, vol. 13, no. 14, 2020, doi: 10.3390/en13143549.

[15] K. Kumar, K. V. V. S. R. Chowdary, P. Sanjeevikumar, and R. Prasad, "Analysis of Solar PV Fed Dynamic Wireless Charging System for Electric Vehicles," *IECON Proceedings (Industrial Electronics Conference)*, vol. 2021-Octob, pp. 1–6, 2021, doi: 10.1109/IECON48115.2021.9589677.

[16] B. Ji *et al.*, "Basic study of solar battery powered wireless power transfer system with MPPT mode and DC bus stabilization for lunar rover," *Proceedings: IECON 2018 - 44th Annual Conference of the IEEE Industrial Electronics Society*, vol. 1, pp. 4787–4792, 2018, doi: 10.1109/IECON.2018.8591152.

[17] A. Mahesh, B. Chokkalingam, and L. Mihet-Popa, "Inductive Wireless Power Transfer Charging for Electric Vehicles-A Review," *IEEE Access*, vol. 9, pp. 137667–137713, 2021, doi: 10.1109/ACCESS.2021.3116678.

[18] G. Buja, M. Bertoluzzo, and K. N. Mude, "Design and Experimentation of WPT Charger for Electric City Car," *IEEE Transactions on Industrial Electronics*, vol. 62, no. 12, pp. 7436–7447, 2015, doi: 10.1109/TIE.2015.2455524.

[19] K. Colak, E. Asa, M. Bojarski, D. Czarkowski, and O. C. Onar, "A Novel Phase-Shift Control of Semibridgeless Active Rectifier for Wireless Power Transfer," *IEEE Trans Power Electron*, vol. 30, no. 11, pp. 6288–6297, 2015, doi: 10.1109/TPEL.2015.2430832.

[20] L. Pamungkas, M. Tampubolon, Q. Lin, and H. J. Chiu, "Performance Comparison of Primary Side PFM and Secondary Side PWM for SS Wireless Power Transfer CC/CV Control Strategy," *Proceedings - 2018 IEEE International Power Electronics and Application Conference and Exposition, PEAC 2018*, pp. 1–5, 2018, doi: 10.1109/PEAC.2018.8590421.

[21] X. Sheng, L. Shi, and M. Fan, "An Improved Pulse Density Modulation of High-Frequency Inverter in ICPT System," *IEEE Transactions on Industrial Electronics*, vol. 68, no. 9, pp. 8017–8027, 2021, doi: 10.1109/TIE.2020.3013782.

[22] H. Li, J. Fang, S. Chen, K. Wang, and Y. Tang, "Pulse Density Modulation for Maximum Efficiency Point Tracking of Wireless Power Transfer Systems," *IEEE Trans Power Electron*, vol. 33, no. 6, pp. 5492–5501, 2018, doi: 10.1109/TPEL.2017.2737883.

[23] A. Karafil, H. Ozbay, and S. Oncu, "Design and Analysis of Single-Phase Grid-Tied Inverter With PDM Mppt-controlled Converter," *IEEE Trans Power Electron*, vol. 35, no. 5, pp. 4756–4766, 2020.

[24] K. Unal, G. Bal, S. Oncu, and N. Ozturk, "MPPT Design for PV-Powered WPT System with Irregular Pulse Density Modulation," *Electric Power Components and Systems*, vol. 51, no. 1, pp. 83–91, 2023, doi: 10.1080/15325008.2022.2161674.

[25] X. Sheng and L. Shi, "An Improved Pulse Density Modulation Strategy Based on Harmonics for ICPT System," *IEEE Trans Power Electron*, vol. 35, no. 7, pp. 6810–6819, 2020, doi: 10.1109/TPEL.2019.2958644.

[26] V. Esteve *et al.*, "Enhanced Pulse-Density-Modulated Power Control for High-Frequency Induction Heating Inverters," *IEEE Transactions on Industrial Electronics*, vol. 62, no. 11, pp. 6905–6914, 2015, doi: 10.1109/TIE.2015.2436352.

[27] A. Karafil, "Comparison of the various irregular pulse density modulation (PDM) control pattern lengths for resonant converter with photovoltaic (PV) integration," *Journal of the Faculty of Engineering and Architecture of Gazi University*, vol. 36, no. 3, pp. 1595–1611, 2021, doi: 10.17341/gazimmfd.685751.

[28] I. Bentalhik *et al.*, "Analysis, Design and Realization of a Wireless Power Transfer Charger for Electric Vehicles: Theoretical Approach and Experimental Results," *World Electric Vehicle Journal*, vol. 13, no. 7, 2022, doi: 10.3390/wevj13070121.

[29] H. Yue, Z. Fang, and Y. Xia, "PDM Control Strategy of Extremely High Gain ICPT System Applying for Electrical Isolation Aimed at Maximum Efficiency," *IECON Proceedings (Industrial Electronics Conference)*, vol. 2022-Octob, pp. 1–6, 2022, doi: 10.1109/IECON49645.2022.9968570.

[30] A. Karafil, H. Ozbay, and S. Oncu, "Comparison of regular and irregular 32 pulse density modulation patterns for induction heating," *IET Power Electronics*, no. August, pp. 1–12, 2020, doi: 10.1049/pel2.12012.

[31] A. Karafil, "Comparison of the various irregular pulse density modulation (PDM) control pattern lengths for resonant converter with photovoltaic (PV) integration," *Journal of the Faculty of Engineering and Architecture of Gazi University*, vol. 36, no. 3, pp. 1595–1611, 2021, doi: 10.17341/gazimmfd.685751.

[32] A. Karafil, H. Ozbay, and S. Oncu, "Design and Analysis of Single-Phase Grid-Tied Inverter With PDM Mppt-controlled Converter," *IEEE Trans Power Electron*, vol. 35, no. 5, pp. 4756–4766, 2020.

BIOGRAPHIES

Cem Kutlu received his Master of Science degree from Dicle University, Turkey, in 2012. His main research areas are power electronics, resonant converters, LED drivers, PV system applications, electric vehicles, wireless power transfer and battery chargers. He is currently studying in the Ph. D. program of Electrical Engineering at Bandırma Onyedi Eylül University, Balıkesir, Türkiye

Harun Özbay Ph. D., Associate Professor. He received his B.S. degree in electrical education from Gazi University, Ankara, Turkey, in 2008, the M.S. degree in electrical education from Gazi University, Ankara, Turkey, in 2011, and Ph. D. degree in electrical and electronics engineering from Karabuk University, Karabuk, Turkey, in 2017. He is working with the Electrical Engineering Department, Bandırma Onyedi Eylül University, Balıkesir, Türkiye, where he is currently an Assistant Professor. His research interests include power electronics, resonant converters, electric machines, grid connected inverters, electric power systems, artificial intelligence, LED drivers, PV system applications, MPPT, electric vehicles and battery charger